Design and Simulation Analysis of Intercell Transformer based on Five-level T-type Inverter

Yu Han[1], Shanshan Wang[1], Xuanxi Liu[1], Hanyoung Bu[1], Dongmin Choi[1],
and Younghoon Cho[1]
[1]The Department of Electrical and Electronics Engineering, Konkuk University, Seoul, Republic of Korea

***Abstract*-- To improve the power density of the five-level T-type inverter, a three-phase intercell transformer (ICT) is proposed. The three-phase ICT is the integration of three separate coupled inductors of the proposed inverter on a single core. The ICT created by the coupled inductor often does not alter the output current but does lessen the current ripple in the windings. It also reduces losses, and with the smaller size, the power factor of the ICTs can be much higher than that of the inductor. The paper analyzes the structure of the six coil core, and an equivalent model of the magnetic circuit is established. The method was optimally analyzed by coupled simulation of Maxwell and Simplorer. Furthermore, this result is further verified in the PSIM simulation.**

***Index Terms*--Five-level T-type Inverter, Intercell Transformer, Coupled Inductor, Maxwell**

I. Introduction

Five-level T-type inverters have become increasingly popular in recent years, particularly in grid-connected photovoltaic power systems. The performance and quality of grid-connected inverters have a significant impact on the grid. Compared with the traditional two-level inverter, the primary advantages of a multilevel inverter include low harmonic output voltage content, high inverter efficiency, suitability for low harmonics, high voltage, and high power output, etc [1].

Additionally, the use of coupled inductors reduces the ripple current and generates higher voltage levels. In addition to the benefits of coupling inductance, the proposed intercell transformer (ICT) can also solve the problem of the inductors growing larger as the power increases[2-4].

Inductor coupling to form an inter-cell transformer (ICT) does not usually change the output current. However, it reduces current fluctuations in the windings and current oscillations in some regions of the core. Especially the monolithic ICT can further reduce weight and size, which is why it was chosen in the current study. However, as the overall control of the circuit and the complexity of the used magnetic couplers lead to the implementation of a limited number of coils, it is difficult to combine more than ten cells.

The inverter used in this paper is shown in Fig. 1. Each phase of the five-level T-type inverter consists of two three-level T-type inverter modules and a coupling inductor. The three-level T-type topology has the advantages of low conductive losses, low switching losses, good output voltage quality, a small number of components, and a straightforward operating principle.

The rest of this paper is presented as follows: Section II describes the topologies and operating principle of the five-level T-type inverter, the types of topologies for monolithic inter-cell transformers, and the design methodology of the proposed ICT. The structure of the six coil ICT core is analyzed, and the equivalent model of the ICT magnetic path circuit is established. Section III presents the Maxwell, Simplorer, and PSIM modeling and simulation analysis of the five-level T-type inverter containing ICT. The simulation results are compared using the finite element method (FEM) software, and the method's validity is determined.

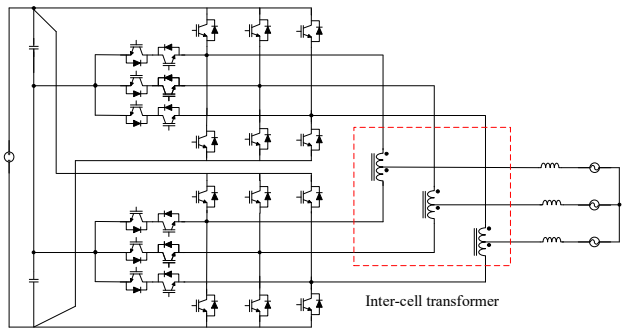

Fig. 1. Five-level T-type inverter.

II. Technical Work Preparation

This section introduces the five-level T-type inverter circuit using the proposed inter-cell transformer and then introduces the topology of the circuit.

A. Five-level T-type Inverter

The five-level T-type inverter with a coupled inductor is shown in Fig. 1. Each phase consists of two parallel three-level T-type inverter legs and a coupled inductor. As shown in Fig. 2(a), in three-level carrier-based modulation, the up and down carrier can be in the same direction or in opposite directions, which is called phase displacement modulation and phase opposite displacement modulation. And the phase displacement modulation method is used here.

The carrier waveforms of inverter leg one and leg two are interleaved by 180°, as shown in Fig. 2(b), The carrier wave for leg 1 is green, and the blue is for leg 2. The outputs of the inverter legs are connected to the coupled inductor to form a single output [5]. In this way, two legs and one coupled inductor together can produce five voltage level lines to the neutral point.

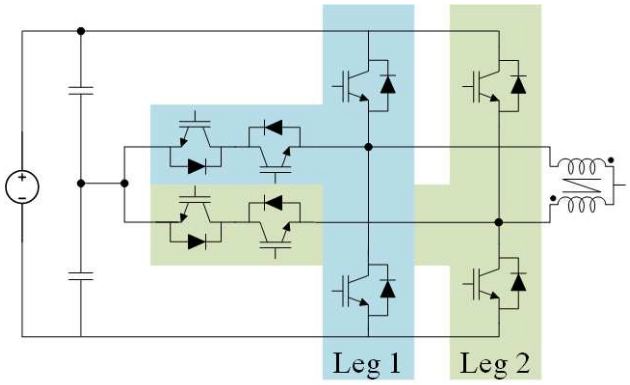

(a)

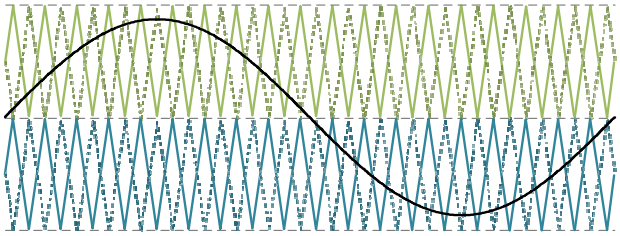

(b)

Fig. 2. Five-level T-type inverter with double ladder ICT. (a) Schemtatic of three Phases. (b) Schematic of one phase.

B. Topology Types of Monolithic Intercell Transformer

There are several ICT topologies with two or more phases. They are usually classified into two different types: monolithic or separate. In the Separate ICT systems, each topology consists of several double-cell transformers connected in different ways. Each winding is connected to a different phase, and the number of separate transformers depends on the topology used.

The monolithic transformer is a type of coupled inductor that puts all windings together in the same magnetic core, as presented in [6-9], and may be divided into three different groups, as shown in Fig. 3:

- Ladder topologies
- Circular topologies
- Circular topologies based on standard cores

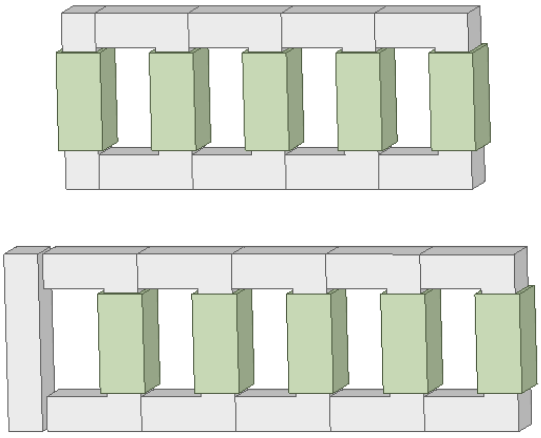

(a)

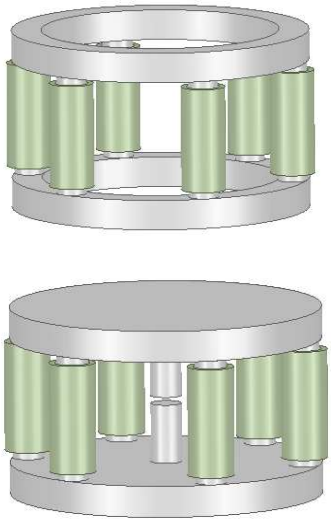

(b)

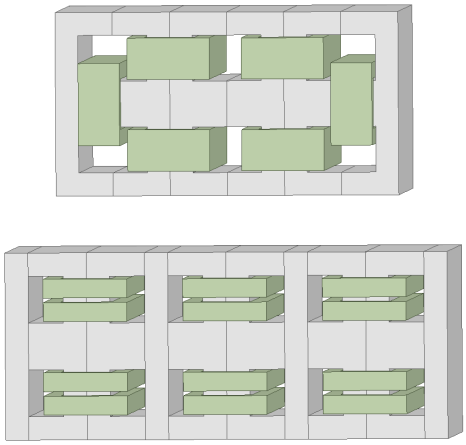

(c)

Fig. 3. Topology types of the Monolithic ICT. (a) Ladder topologies. (b) Circular topologies. (c) Circular topologies based on standard cores.

A topology called double ladder type topology is also feasible. It belongs to the circular topologies but is a more realistic ICTs because it can be assembled more easily.

The proposed three-phase ICT belongs to the double ladder type, and it integrates three separate coupled inductors of the inverter on a set of rectangular-shaped cores of the monolithic type.

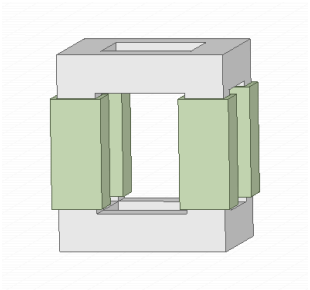

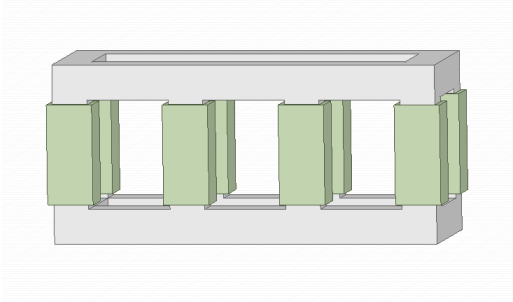

Fig. 4. Double ladder type topology.

C. Intercell Transformer Design

In order to decrease the size of the magnetic components and increase the power density of the inverter, three coupled inductors are integrated into a structure of six U-shaped magnetic cores. Monolithic ICT is a k-phase magnetic device. It uses a monolithic magnetic core with k winding legs (or columns) connected by 2k linking legs. To obtain proper electrical balance, the ICT must be quasi-symmetric, and the core assembly needs to be as simple as possible [10-13]. Therefore, the "double ladder" structure was chosen to use.

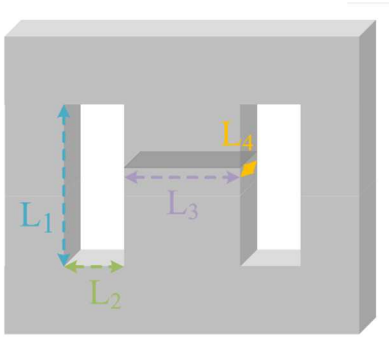

(a)

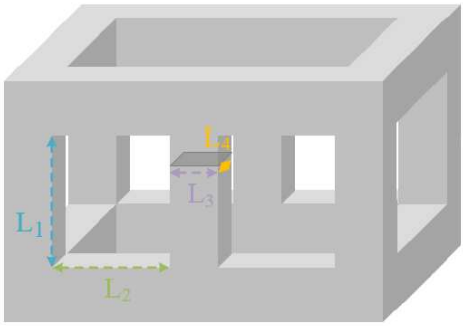

(b)

Fig. 5. Magnetic core structure.
(a) Coupled inductor. (b) Double ladder ICT.

Fig. 5 shows the core structure of one group of coupled inductors (a) and ICT (b). L_1 and L_2 in the figure are the length and width of the core window, L_3 and L_4 are the length and width of the effective cross section of the core, respectively.

The air gap is often designed in the core of the coupled inductor but not in ICT. Because air gaps are usually not designed in ICT because it causes high magnetizing currents, which increases output current ripple. It can also increase copper losses through induced high frequency currents in the winding conductors close to the air gap.

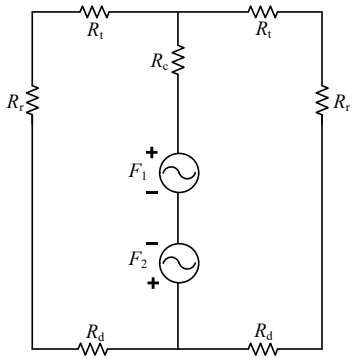

(a)

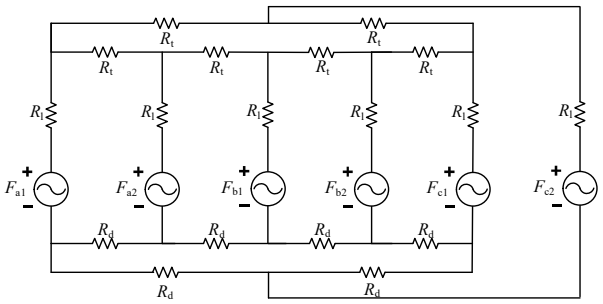

(b)

Fig. 6. Equivalent magnetic circuit.
(a) Coupled inductor. (b) Double ladder ICT.

Fig. 6 shows the equivalent magnetic circuit of the three-phase ICT and one group of EE coupled inductors. A design method based on the area product proposed in Fig. 7 is adopted [14-16]. The area product is the product of the effective cross section of the core A_c and the area of each of the windows in the cell structure A_w. It is often used in inductor designs, as shown in Equations (1-3).

$$A_w = L_1 L_2 \tag{1}$$

$$A_c = L_3 L_4 \tag{2}$$

$$A_w A_c = \frac{P}{k} \frac{K_P K_W}{\Delta B_M (A_W A_C) J (A_W A_C) F} \tag{3}$$

Where J_{rms} is the rms current density, K_w is the winding ratio, which is the ratio of window area to copper section. K_P is the power coefficient depending on the converter topology.

$$\Delta B_M = B_{sat} - B_{dc} \tag{4}$$

Where B_{sat} is the saturation induction.

The formula for inductance is

$$L_M = \frac{N^2}{R_m} \tag{5}$$

Where the equivalent reluctance of the inductor is R_m, and the number of turns of the coil is N.

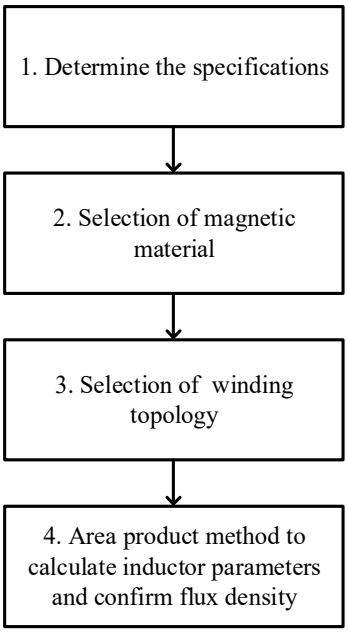

Fig. 7. Design block diagram.

The results of the ICT design will be analyzed by three main models according to two different conditions to compare the ripple size.

They are three sets of EE core coupled inductors and the proposed ICT. Furthermore, as a comparison group, three new coupled inductor sets were modeled based on the volume of the ICT.

III. MODELING AND SIMULATION

To verify the accuracy of the design, finite element coupling simulations were performed using Maxwell and simplorer software. As depicted in Fig. 8, the general EE coupled inductors (3 groups) and the proposed ICT were modeled and simulated separately. The physical model is constructed under ANSYS Maxwell-3D Transient solver. The external circuit excitation sources in ANSYS Simplorer are loaded into the model.

And the results were compared. Fig. 9 shows the modeling of the proposed three-phase ICT and generally coupled inductor. The ICT consists of six U-shaped cores with core type UU6481 and 18 turns. The material of the core uses FM4 ferrite with characteristics such as low power loss, high B, and high frequency. While the EE coupled inductor uses two stacks of EE8076S cores with 23 turns.

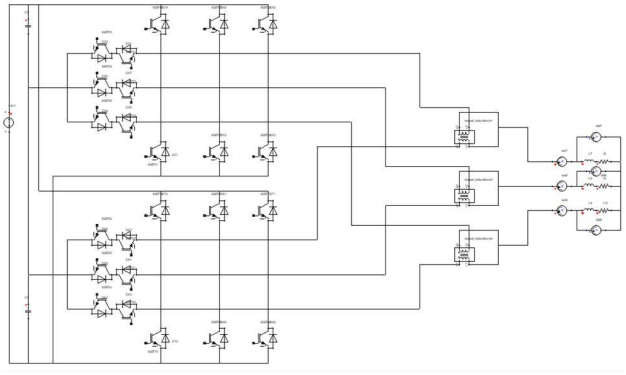

(a)

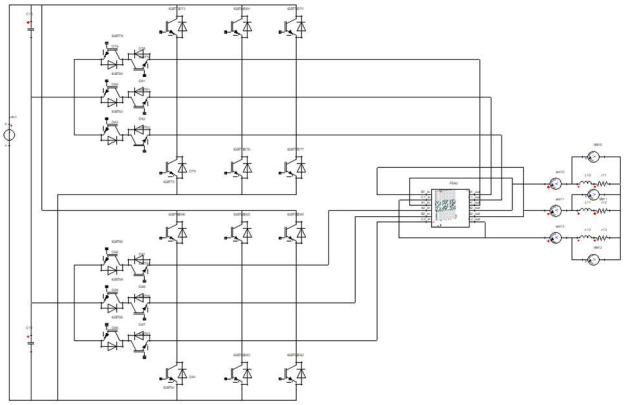

(b)

Fig. 8. Coupling simulation diagram of Maxwell software and Simplorer.

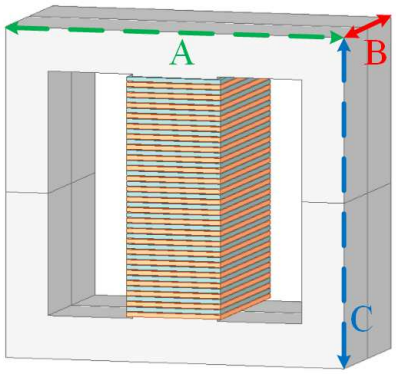

(a)

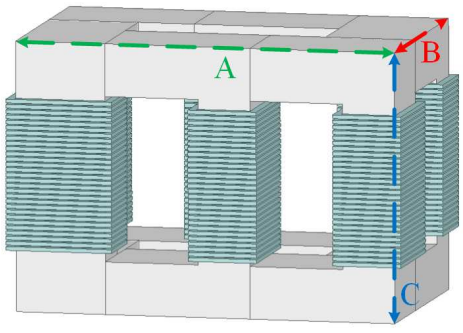

(b)

Fig. 9. Simulation modeling.
(a) Coupled inductor. (b) Double ladder ICT.

The dimensions and simulation inductance values of the two inductors, the proposed ICT and EE coupled inductor I, are shown in Table I, The Length, Width, and Height in the table represent the values of A, B, and C in Fig. 4. indicate that the dimensions of ICT are much smaller than those of the EE coupled inductor under similar inductance conditions.

To further demonstrate the advantage of the proposed ICT, the volume of ICT was used as the total volume of the new Three groups EE coupled inductor under the existing ICT numerical conditions. This means that the volume of the new coupled inductor is one-third of the ICT volume as the dimensional data. The new EE coupled inductor II was designed and modeled, and the parameters are also shown in the table below, with an inductance much lower than the ICT.

TABLE I
INDUCTOR PARAMETERS

PARAMETER	ICT	Coupled Inductor I (per set)	Coupled Inductor II (per set)
Length [mm]	105.20	80.00	64.70
Width [mm]	64.70	76.00	64.00
Height [mm]	64.00	40.00	35.07
Inductance [mH]	7.41	7.28	2.82

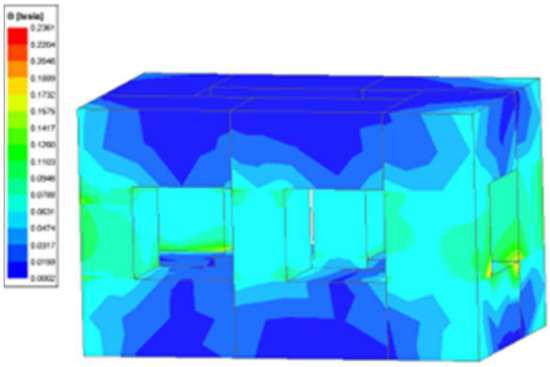

Fig. 10. Distribution of magnetic flux density in ICT core.

The flux density distribution of each magnetic circuit of the ICT core is simulated. Fig. 10 shows the Maxwell and Simplorer simulation analysis results of magnetic field density. The maximum value is 0.24, which does not exceed the maximum value of the core.

The circuit simulation for both inductor cases was then verified using PSIM software. Fig. 11 shows the circuit and current waveform results of the simulation. The results show that the ripple of ICT is smaller compared to the general EE coupled inductor I for similar inductance values. For the same volume, the inductance of ICT is larger than that of coupled inductor II, and the ripple is smaller.

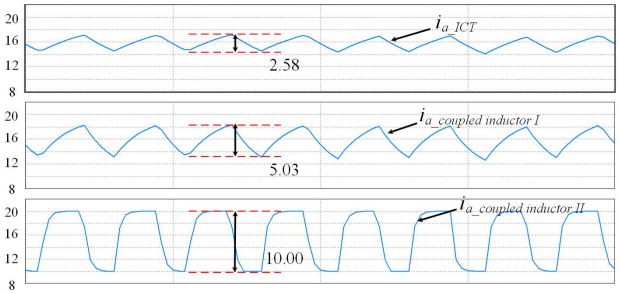

Fig. 11. The circuits and current waveforms of PSIM simulation.

IV. CONCLUSION

This paper presents a method to increase the power density of a five-level T-inverter using a double ladder intercell transformer. This results in reducing the size of the coupling inductor itself and improving the effectiveness of the dynamics. The modeling simulations of the ICT and EE coupled inductors are compared for the same inductance and size, and respectively This was demonstrated and verified by FEA and PSIM simulations.

ACKNOWLEDGMENT

This work was supported by Korea Institute of Energy Technology Evaluation and Planning (KETEP) grant funded by the Korea goverment (MOTIE) (20212020800020, Development of High Efficiency Power Converter based on Multidisciplinary Design and Optimization Platform).

REFERENCES

[1] Shi, Y., Wang, L., Xie, R., Shi, Y., & Li, H, "A 60-kW 3-kW/kg Five-Level T-Type SiC PV Inverter With 99.2% Peak Effificiency," IEEE Transactions on Industrial Electronics, vol. 64, no. 11, pp. 9144 - 9154, 2017.

[2] Hanafi, Salah, et al, "Control of parallel multicellular DC/AC converter including monolithic inter-cell transformer in a real-time environment," REVUE ROUMAINE DES SCIENCES TECHNIQUES—SÉRIE ÉLECTROTECHNIQUE ET ÉNERGÉTIQUE 66.3, pp.169-174,2021.

[3] Park, Ki-Bum, et al., "Optimization of LCL Filter With Integrated Intercell Transformer for Two-Interleaved High-Power Grid-Tied Converters," IEEE Transactions on Power Electronics, vol. 35, no. 3, pp. 2317-2333, 2020.

[4] Ewanchuk, Jeffrey, and John Salmon, "Three-limb coupled inductor operation for paralleled multi-level three-phase voltage sourced inverters," IEEE Transactions on Industrial Electronics 60.5, pp.1979-1988,2012.

[5] Bernardo Cougo, "Parallel Three-Phase Inverters: Optimal PWM Method for Flux Reduction in Intercell Transformers," IEEE Transactions on Power Electronics., vol. 26, no. 8, pp. 2184 - 2191, 2011.R. Nicole.

[6] B. Cougo, "Design and optimization of intercell transformers for parallel multicell converters," PhD Thesis, University of Toulouse, INP, LAPLACE Laboratory, Toulouse, France, 2010

[7] Costan, Valentin, “Convertisseurs parallèles entrelacés: étude des pertes fer dans les transformateurs inter-cellules,” Diss. 2007.
[8] Meynard, T., Cougo, B., Forest, F., & Labouré, E, “Parallel multicell converters for high current: Design of intercell transformers,” In: 2010 IEEE International Conference on Industrial Technology. IEEE, pp. 1359-1364, 2010.
[9] Le, Trong Trung, et al, “Influence of cold isostatic pressing on the magnetic properties of Ni-Zn-Cu ferrite,” AIP Advances 8.4 (2018): 047806.
[10] Forest, F., Meynard, T. A., Huselstein, J. J., Flumian, D., Rizet, C., & Lacarnoy, A, “Design and characterization of an eight-phase-137-kW intercell transformer dedicated to multicell DC–DC stages in a modular UPS,” IEEE transactions on power electronics 29.1, pp.45-55, 2010.
[11] F. Forest, E. Labour´e, T. Meynard, and M. Arab, “Analytic design method based on homothetic shape of magnetic cores for high-frequency transformers,” IEEE Transactions on Power Electronics 22.5, pp.2070-2080, 2007.
[12] Sanchez, S., Risaletto, D., Richardeau, F., Meynard, T., & Sarraute, E., “Pre-design methodology and results of a robust monolithic Inter Cell Transformer (ICT) for parallel multicell converter,” IECON 2013-39th Annual Conference of the IEEE Industrial Electronics Society. IEEE, 2013.
[13] McLyman, Colonel Wm T, “Transformer and inductor design handbook,” CRC press, 2004.
[14] Laka, A., Barrena, J. A., Chivite-Zabalza, J., & Rodriguez-Vidal, M., “Parallelization of two three-phase converters by using coupled inductors built on a single magnetic core,” Przegląd Elektrotechniczny, 89(3a), pp.194-198,2003.
[15] Forest, F., Meynard, T. A., Laboure, E., Costan, V., Sarraute, E., Cuniere, A., & Martire, T., “Optimization of the supply voltage system in interleaved converters using intercell transformers,” IEEE Transactions on Power Electronics, 22(3) , pp.934-942,2007.
[16] Yugang, Y., Dong, W., & Kaiqiang, Z., “Design and application of the “UUUU” shape coupled inductor,” Transactions of China Electrotechnical Society, 31(5), pp.35-43,2016.